Bloch oscillations of atoms, adiabatic rapid passage, and monokinetic atomic beams

Ekkehard Peik,* Maxime Ben Dahan, Isabelle Bouchoule, Yvan Castin, and Christophe Salomon
Laboratoire Kastler Brossel, Ecole Normale Supérieure, 24 rue Lhomond, 75231 Paris Cedex 05, France
(Received 18 July 1996)

We study the dynamics of ultracold atoms in a periodic optical potential submitted to a constant external force. Bloch oscillations in the fundamental and first excited bands of the potential are observed. In addition to a solid-state analysis we give a quantum-optics interpretation of this effect in terms of photon exchanges between the atoms and the laser waves. The dynamics of Bloch oscillations are equivalent to a sequence of adiabatic rapid passages between momentum states and can be described using the dressed-atom approach. We demonstrate efficient and dissipation-free acceleration of atoms by coherent transfer of a large number of photon momenta (≈ 100). This technique produces atomic beams with a very small longitudinal velocity spread that may find applications in atom optics and precision measurements. [S1050-2947(97)03504-X]

PACS number(s): 32.80 Pj, 03.75.−b, 03.65.−w

I. INTRODUCTION

Manipulation of atoms with lasers has progressed considerably in the last decade [1]. In this paper, we analyze the behavior of ultracold atoms in the light field of two counterpropagating laser waves. When these waves are detuned far from any atomic resonance, the light shift of the ground state leads to a conservative periodic potential with spatial period $\lambda/2$, half the laser wavelength. This configuration was first used in the context of atom diffraction [2] leading to the development of atom-optics elements, interferometry [3,4], or studies of quantum chaos [5]. We use Raman subrecoil laser cooling techniques [6,7] to prepare the atoms with a momentum spread δp smaller than the photon momentum $\hbar k$ in the direction of the optical lattice. The corresponding coherence length $h/\delta p$ thus extends over several periods of the potential.

If the two counterpropagating waves have a time-dependent frequency difference they form a ''standing wave'' in a moving reference frame. If, in addition, the frequency difference varies linearly with time, the reference frame in which the optical potential is stationary is uniformly accelerated. In this frame the atoms experience a constant inertial force in addition to the force induced by the optical potential. As shown in recent papers [8,9], this simple system ''atom+moving standing-wave'' models quite well the case of electrons in a perfect crystal under the influence of a constant electric field [10–12]. For instance, Bloch oscillations (BO) of atoms in a light lattice [8], as well as Wannier-Stark ladders [9], have recently been observed.

These experiments have been made possible thanks to several differences that exist between electrons in solids and atoms prepared in an optical potential. (i) The initial momentum distribution of atoms is well defined, can be tailored at will, and can be much narrower than h/a, where a is the lattice period. By adiabatically switching on the optical potential, this narrow momentum distribution is turned into a statistical mixture of Bloch states in a given energy band with a quasimomentum width $\delta q = \delta p/\hbar$ much smaller than the width $2\pi/a$ of the Brillouin zone. (ii) The periodic potential, being created by light, can be easily turned on and off. With sudden switch-off we can directly measure the momentum distribution of Bloch states [8]. (iii) There is virtually no scattering from defects of the potential or from interactions between particles. (iv) Bloch oscillations in the time domain can have periods in the millisecond range, i.e., ten orders of magnitude longer than in semiconductors [13–16].

Because the periodic optical potential has its origin in photon redistribution between the two counterpropagating laser waves, we can develop a ''quantum-optics'' description of the atomic motion in a frequency-chirped standing wave without reference to solid-state concepts, such as band theory. This description, which is equivalent to the Bloch formalism, offers new insights into the physical phenomena. In the nondissipative case, the momentum of the atoms, in the laboratory frame, can only change in units of $2\hbar k$ via absorption from one wave and stimulated emission into the other. The dynamics is thus conveniently described in terms of Raman transitions between momentum states, occuring when the frequency difference between the two waves fulfills the energy-conservation condition. The increasing frequency difference leads to a succession of adiabatic rapid passages between momentum states differing by $2\hbar k$, resulting in a coherent acceleration of the atoms in the laboratory frame. We will show the connection with the recoil-induced resonances, which have been recently observed for atoms trapped in *dissipative* optical lattices [17] in which the momentum spread is several times greater than $\hbar k$ [18].

The coherent acceleration of the atoms associated with the Bloch oscillations or equivalently with the successive adiabatic rapid passages, is a new tool for producing atomic beams with a very narrow momentum distribution in the propagation direction [19]. For instance, we have been able in preliminary experiments, to accelerate a cloud of cesium atoms to an average momentum of $80\hbar k$ while maintaining the initial momentum spread of $\hbar k/4$ along the standing-wave direction.

We have organized our paper in the following way: in Sec. II, we give a detailed description of the experimental setup. Then in Sec. III, following Ref. [8], we analyze our

*Present address: Max-Planck-Institut für Quantenoptik, Hans-Kopfermannstr. 1, D-85748 Garching, Germany.

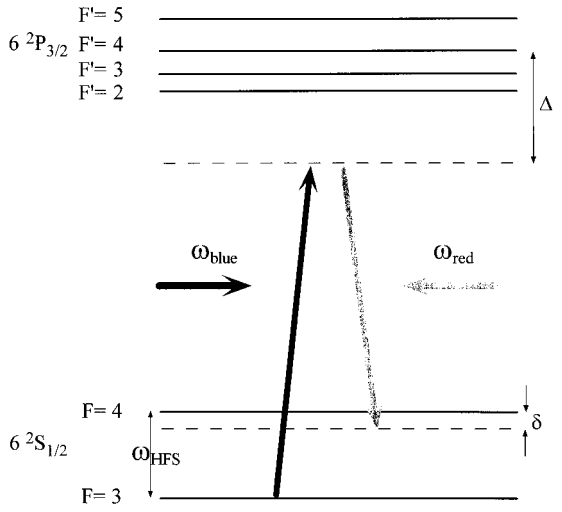

FIG. 1. Cesium energy levels and Raman beams for subrecoil cooling. The high-frequency Raman beam (at ω_{blue}) is also used to create the chirped standing wave for the Bloch oscillations. Δ is typically 30 GHz, such that direct excitation of the $^2P_{3/2}$ state is negligible during the 20 ms interaction time.

experiments in terms of atoms in a periodic potential induced by light under the influence of a constant force. We present our results on Bloch oscillations in the fundamental band and compare Bloch oscillations in the fundamental and the first excited band. In Sec. IV we give a quantum optics description of Bloch oscillations using the concepts of adiabatic rapid passage and Landau-Zener transitions. Bloch oscillations are also depicted in the dressed-atom basis. Finally, in Sec. V, we apply the previous analyses to the coherent acceleration of cold atomic wave packets and present experimental results.

II. EXPERIMENTAL SETUP

The experimental apparatus consists of a vapor-cell magneto-optical trap (MOT) for cesium atoms [20], a laser system for loading the trap and precooling the atoms in optical molasses [1,21], and a laser system for Raman cooling [6,7,22] and for generating the chirped standing wave. All lasers employed in the experiment are diode lasers, operating on wavelengths close to the cesium $6S_{1/2}\rightarrow 6P_{3/2}$ transition at 852 nm (cf. Fig. 1). Part of this setup has been used in previous experiments on Raman cooling of cesium [7,22].

The cesium cell is a hollow glass cube of 12 cm side-length, antireflection coated on the outside and pumped by a 25 l/s ion-getter pump. The cesium vapor pressure is on the order of 10^{-8} mbar, providing about 10^8 atoms into the MOT in a loading time of 500 ms. The cell together with the magnetic-field coils of the MOT is placed in a two-layer mumetal shield, surrounded by a set of three pairs of large compensation coils. After loading the MOT, the field is switched off and allowed to decay in a time of 200 ms. During this period the atoms are cooled in an optical molasses to a momentum spread of $5\hbar k$, corresponding to a temperature of 6μK. When Raman cooling is begun after the molasses period, the magnetic field has decreased to a value on the order of 100 μG. Raman cooling and interaction with a chirped standing wave are performed while atoms are in

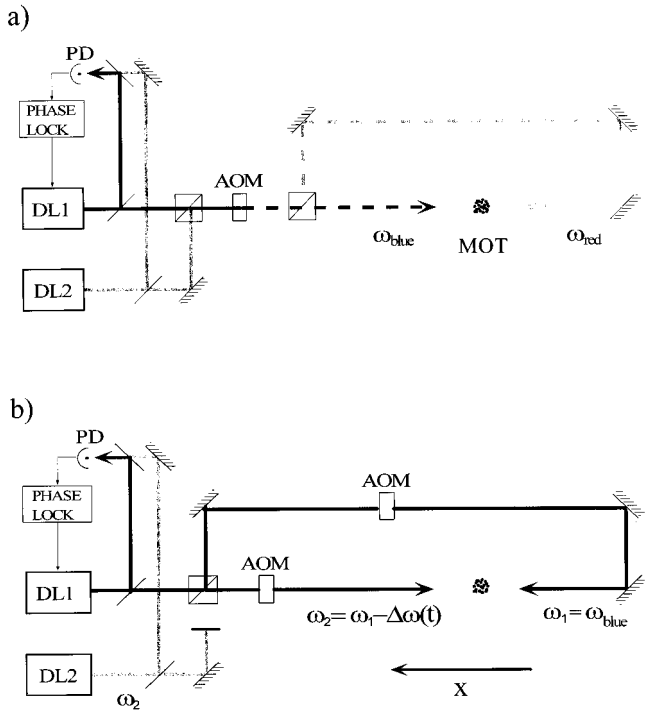

FIG. 2. (a) Magneto-optical trap and Raman beams used for subrecoil cooling and probing of the momentum distribution of Bloch states in the laboratory frame. The frequency difference of the two laser diodes DL_1 and DL_2 is phase locked to a tunable frequency source near the cesium ground-state hyperfine frequency. (b) After the subrecoil cooling phase, the beam of DL_2 is blocked and the beam of DL_1 is passed through AO modulators to produce the chirped standing wave.

free fall under gravity. The diameter of the horizontal laser beams limits our interaction time to 25 ms.

The laser system for the MOT and optical molasses consists of a master laser, frequency narrowed by feedback from an external Fabry-Pérot cavity and locked to a saturated absorption resonance in a small cesium cell. The different detunings from the $6S_{1/2},F=4\rightarrow 6P_{3/2},F=5$ resonance for the MOT and molasses are controlled using an acousto-optical modulator (AOM). The radiation from this frequency stable laser is used to inject a 150 mW slave diode laser, whose output is spatially filtered and separated into the six beams required for the MOT. Repumping radiation on the $6S_{1/2},F=3\rightarrow 6P_{3/2},F=4$ line is provided by a third diode laser, frequency stabilized by feedback from an optical grating. During the Raman cooling phase and the chirped standing-wave phase, all these beams are blocked by mechanical shutters and their AOMs are turned off to avoid any light shift due to near resonant photons. To drive the Raman transition between the two hyperfine ground states of the cesium atom, two grating stabilized extended cavity diode lasers are optically phase locked at a frequency offset of 9.192 GHz [23], as shown in Fig. 2. The detuning of these lasers from the $6S_{1/2},F=4\rightarrow 6P_{3/2},F=5$ line is measured by observing the beat note between one of them and the laser that provides the radiation for the MOT. We typically worked at a detuning Δ of 30 GHz, a value corresponding to about 5700 natural linewidths Γ of the cesium transition and larger than the hyperfine splittings of both the excited and

the ground state. This detuning is sufficiently large to avoid excitation of the $6P_{3/2}$ level, which would be followed by the random momentum transfer due to the spontaneous emission of a photon. It also reduces the differential light shifts between the Zeeman sublevels of the ground state. This is essential for our method of Raman cooling using square pulses [7] and for the observation of BO, where all the atoms should experience the same light shift potential, irrespective of their magnetic quantum state.

Each of the two Raman beams is amplified by injection locking of a high power diode laser (200 mW). The two beams are superimposed, passed through an AOM that controls the envelope of the Raman pulses, a spatial filter, a Pockels cell, and a polarizing beam splitter. The latter are used to exchange the directions of the two beams and, hence, the sign of the transfered momentum. The two beams finally pass the cesium cell with a diameter at $1/\sqrt{e}$ intensity of 6 mm, a peak intensity of 70 mW/cm^2 and having orthogonal linear polarizations. They are superimposed antiparallel to each other and aligned horizontally with a precision of about 5' (cf. Fig 2). A distributed Bragg reflector (DBR) laser diode stabilized on the $6S_{1/2},F=4\rightarrow 6P_{3/2},F=4$ transition is used to pump the atoms back to the $F=3$ ground state after each Raman transfer. In order to diminish its sensitivity against parasitic external feedback we use this diode in an extended cavity configuration with controlled feedback from a piezo-mounted partial reflector. This beam is superimposed on one of the MOT axes and makes an angle of 3° with the Raman beams. With an intensity of 20 mW/cm^2, pulses with a duration of 10 μs were used to effectively repump all the atoms.

The chirped standing wave is generated from the Raman laser having the higher frequency (cf. Fig. 2). Its output is split into two beams that pass through two acousto-optical modulators and spatial filters. One of these AOMs is driven by a quartz oscillator at a fixed frequency of 80 MHz, and the other by a variable radio frequency obtained by mixing a quartz oscillator at 60 MHz with the output of an arbitrary-function generator around 20 MHz. The system allows us to turn on the two beams with a variable rise time (on the order of 200 μs), to apply a frequency ramp with variable slope, and to finally turn the beams off fast (within 1 μs). The frequency difference is controlled by monitoring the beat note between the two AOM drives. The two beams have a diameter at $1/\sqrt{e}$ intensity of 4.5 mm, a peak intensity of 40 mW/cm^2 and parallel linear polarizations. They are superimposed onto the horizontal optical axis of the Raman beams in counterpropagating directions.

Derived from the MOT laser is a vertical probe beam, composed of two counterpropagating waves having the same circular polarization. It is used to excite the $6S_{1/2},F=4\rightarrow 6P_{3/2},F=5$ transition, so that the number of atoms in the $F=4$ ground-state hyperfine level can be measured via the detected fluorescence signal on a photodiode. The velocity distribution of the atoms is probed by velocity selective Raman transitions: the Raman beams are counterpropagating and a Raman pulse first transfers one velocity class of the $F=3$ atoms to the otherwise empty $F=4$ level. Then the probe beam measures the number of atoms in $F=4$. This sequence (Raman pulse-probe beam) is repeated while scanning the detuning of the Raman lasers in order to record the atomic velocity distribution.

III. BLOCH OSCILLATIONS

In this section we analyze our experimental situation in terms of a particle in a one-dimensional (1D) periodic potential submitted to a constant force. This problem corresponds, for instance, to electrons in a crystal under the influence of a constant homogeneous electric field. This situation, originally studied by Bloch [10] in the late twenties led to the prediction of striking phenomena [11]. This ''solid-state analysis'' is the point of view we have chosen in Ref. [8]. We recall here the main aspects, with some additional comments, and present our experimental results.

A. Theory

Let us first consider the case where no external force is applied on the particle. The Hamiltonian of the particle is, thus, simply

$$H=\frac{p^2}{2m}+V(x), \tag{1}$$

where m is the mass of the particle and V satisfies $V(x+a)=V(x)$ (a is the period of the potential). The properties of the eigenstates and eigenenergies of this Hamiltonian are usually derived from the Bloch theorem [24]. This theorem states that the eigenenergies $E_n(q)$ and the eigenstates $|n,q\rangle$ of H are labeled by: (i) a discrete band index n, (ii) a continuous quasimomentum q. The eigenfunctions Ψ can be written

$$\Psi_{n,q}(x)=\langle x|n,q\rangle=e^{iqx}u_{n,q}(x), \tag{2}$$

where $|u_{n,q}\rangle$ is spatially periodic with the periodicity a of the lattice and satisfies the Schrödinger equation

$$H_q|u_{n,q}\rangle=E_n(q)|u_{n,q}\rangle \quad \text{with } H_q=\frac{(p+\hbar q)^2}{2m}+V(x). \tag{3}$$

Furthermore, $|n,q\rangle$ and $E_n(q)$ are periodic functions of the quasimomentum q with period $2\pi/a$ and q is, thus, conventionally reduced to the first Brillouin zone $]-\pi/a,+\pi/a]$. All these results can be collected in a band structure which is simply the energy spectrum of the particle (Fig. 3).

If a constant and spatially uniform force F is suddenly applied to the particle for $t>0$, the initial Bloch state $|n,q\rangle$ is no longer an eigenstate of the resulting Hamiltonian

$$H'=\frac{p^2}{2m}+V(x)-Fx. \tag{4}$$

However, the Bloch form [Eq. (2)] for the wave function is preserved

$$\Psi(x,t)=e^{iq(t)x}u(x,t) \tag{5}$$

with a time-dependent quasimomentum $q(t)$ given by

$$q(t)=q(0)+Ft/\hbar \tag{6}$$

and a spatially periodic part evolving as

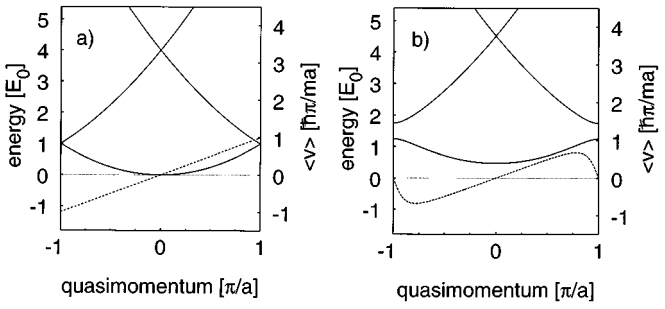

FIG. 3. Band structure $E_n(q)$ (solid line) for a particle in a periodic potential $U(x)=U_0\sin^2\pi x/a$ and mean velocity $\langle v\rangle_0(q)$ in the fundamental band (dashed line): (a) free particle case, (b) $U_0=E_0=\hbar^2\pi^2/2ma^2$. A gap opens at $q=\pm\pi/a$. Under the influence of a weak uniform force, a particle prepared in the fundamental band remains in this band and performs a motion periodic in time called a Bloch oscillation.

$$i\hbar\frac{d}{dt}|u(t)\rangle=H_{q(t)}|u(t)\rangle. \tag{7}$$

Furthermore, when F is weak enough not to induce interband transitions the adiabatic approximation can be applied to Eq. (7). In this case $|u(t)\rangle$ is equal to $|u_{n,q(t)}\rangle$ up to the phase factor $\exp[-i\int_0^t d\tau E_n(q(\tau))/\hbar]$. Since the quasimomentum Eq. (6) scans the reciprocal lattice with uniform speed, the wave function $\Psi(x,t)$ is periodic in time with a period

$$\tau_B=\frac{h}{|F|a}, \tag{8}$$

corresponding to a $2\pi/a$ shift for the quasimomentum or equivalently to a full scan of the first Brillouin zone. The mean velocity of the particle in state $|n,q(t)\rangle$,

$$\langle v\rangle_n(q)=\frac{1}{\hbar}\frac{dE_n(q)}{dq}, \tag{9}$$

is a periodic function of q as $E_n(q)$. Since q evolves linearly in time, $\langle v\rangle_n(t)$ is an oscillatory function with zero mean value. These so-called ''Bloch oscillations'' have never been observed in a natural lattice for electrons in a dc electric field, because the coherent evolution is limited to a tiny fraction of the Brillouin zone by collisions with lattice defects or impurities [13]. However, this effect has been recently observed in semiconductor superlattices [14–16].

In order to observe BO it is crucial that the force F remains weak enough not to induce interband transitions. We apply the usual adiabaticity criterion [25] to Eq. (7)

$$\left|\left\langle u_{n,q}\left|\frac{d}{dt}\right|u_{n',q}\right\rangle\right|\ll|E_n(q)-E_{n'}(q)|/\hbar(n\neq n'). \tag{10}$$

Taking the derivative of Eq. (3) with respect to q we obtain (as in [24]) $\langle u_{n,q}|\,\mathrm{d}/\mathrm{d}q\,|u_{n',q}\rangle=\langle u_{n,q}|\hbar p/m|u_{n',q}\rangle/[E_{n'}(q)-E_n(q)]$, for $n\neq n'$. Condition (10) then imposes for the fundamental band and $q=k$ (the most critical point) $|ma\lambda/2|\ll(\pi/8)U_0^2/E_R$ in the perturbative regime $U_0\leqslant 10E_R$. One could think of increasing the potential depth in order to make the condition (10) easier to satisfy. This would, however, flatten the lowest bands, thus reducing the amplitude of the oscillations and making it difficult to measure. On the other hand, a minimal force is required to scan the whole first Brillouin zone in the limited time of the experiment, thus imposing a lower limit on the potential depth.

As described in [8], our periodic potential results from the light shift of the ground state of atoms in the light field of a one-dimensional linearly polarized standing wave provided by two counterpropagating beams with equal intensity. All Zeeman sublevels of $F=3$ are equally shifted and the corresponding potential is equal to

$$U(z)=U_0\sin^2(kx)=\frac{U_0}{2}[1-\cos(2kx)], \tag{11}$$

with

$$U_0=(2/3)\hbar\Gamma(I/I_0)(\Gamma/\Delta), \tag{12}$$

where I is the laser intensity in one beam and $I_0=2.2$ mW/cm^2 is the saturation intensity. This potential is periodic with spatial period $\lambda/2$ corresponding to a first Brillouin zone extending in the reciprocal lattice between $-\pi/(\lambda/2)=-k$ and $+\pi/(\lambda/2)=+k$. The natural energy scale is then the recoil energy $E_R=(\hbar k)^2/2m$. In our experiments, the potential depth is adjustable up to about 20 E_R. Resonant excitation to $6P_{3/2}$ and subsequent spontaneous emission depends on laser intensity and detuning and thus, for large enough detuning, dissipation can be made negligible. For typical conditions ($U_0=5E_R$ and $\Delta=30$ GHz), the mean excitation rate per atom is 4 s^{-1}. The excitation probability is very small during the 25 ms interaction time.

If we introduce a tunable frequency difference $\Delta\nu(t)$ between the two waves, the light field is no longer a standing wave in the laboratory frame. For a constant frequency difference, this corresponds to a uniform drift while for a difference linear in time the standing wave is stationary in an *accelerated* frame. In this frame, the atoms thus experience a constant inertial force in addition to the effect of the periodic potential (Appendix)

$$F=-ma=-m\frac{\lambda}{2}\frac{d}{dt}\Delta\nu(t)=-\frac{m}{2k}\frac{d}{dt}\Delta\omega(t). \tag{13}$$

B. Experimental sequence

In our experiments we first perform Raman subrecoil cooling, which is essential to produce an initial velocity distribution with a width smaller than the extension of the first Brillouin zone [6,22,7]. Equivalently, one can say that the coherence length $h/\delta p$ of the atoms extends over several periods $a=\lambda/2=\pi/k$ of the potential, i.e., the atoms really experience a periodic potential. Furthermore, as shown in Fig. 4 and in [8], amplitudes of the BO in the fundamental band are less than a recoil velocity making it impossible to detect with a broad molasses velocity distribution. Here we have used 1D Raman cooling with square pulses [7] to prepare atoms in 12 ms in a narrow peak with a nearly Lorentzian line shape of half width at half maximum of $0.24v_R$ (where v_R is the recoil velocity $\hbar k/m=3.5$ mm/s).

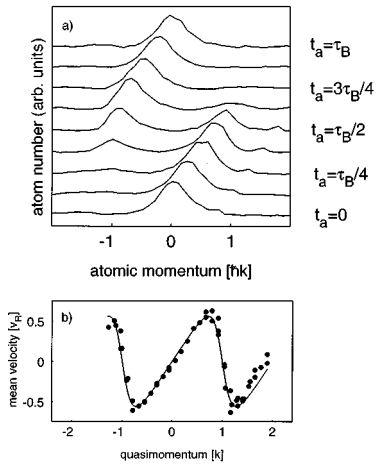

FIG. 4. Bloch oscillations of atoms in the fundamental band: (a) momentum distribution of Bloch states in the accelerated frame for equidistant values of the acceleration time t_a between $t_a=0$ and $t_a=\tau_B=8.2$ ms. (The small peak in the right wing of the first five spectra is an artifact created by a stray reflection of the Raman beams on the cell windows). (b) Mean atomic velocity in units of the photon recoil velocity v_R. Solid line: theory. The light potential depth is $U_0=2.3E_R$ and the acceleration is $a=-0.85$ m/s^2.

We then adiabatically turn on the potential by linearly increasing the intensity of the standing wave with a rise time of about 200 μs. This duration is much longer than the adiabatic limit given by a criterion similar to Eq. (10) in which the time dependence comes from the rate of change of U_0 rather than from $q(t)$. We can thus prepare a statistical mixture of Bloch states around $q=0$ with a width of $q/4$ in the fundamental band. The control of the initial state appears to be a great advantage compared to solid-state experiments. We can actually prepare Bloch states with nearly any initial quasimomentum in any band by introducing a constant frequency shift $\Delta\nu$ between the two waves while we turn on the potential. In the standing-wave frame the atoms are moving with velocity $v_0=-(\Delta\nu)\lambda/2$. If the absolute value of mv_0 is between $n\hbar k$ ($n=0,1,2,\ldots$) and $(n+1)\hbar k$, the corresponding Bloch state lies in the nth band. The quasimomentum is $q_0=mv_0/\hbar\pm(n+1)k$ for odd n and $q_0=mv_0/\hbar\pm nk$ for even n. $+$ and $-$ correspond, respectively, to negative and positive values of v_0. This is not valid for the zone boundaries $[mv_0=\pm(n+1)\hbar k]$ where levels are initially degenerate, making it impossible to prepare the atoms in a single band.

We apply a constant force for various times t_a limited to 8 ms and finally switch off the potential abruptly ($\simeq 1\mu$s). In this way the atoms keep the velocity distribution of the final Bloch states, which can then be measured using the Raman technique [6]. This is a second important difference with solid-state physics in which the effect of the periodic potential cannot be turned off. In our experiments, the Raman velocity selective transitions allow a resolution of about $v_R/18$, much smaller than the extension of the Brillouin zone and the initial momentum spread. This measurement provides the velocity distribution in the laboratory frame. The distribution in the accelerated frame is simply obtained from the distribution in the laboratory frame by a translation of $-mat_a$.

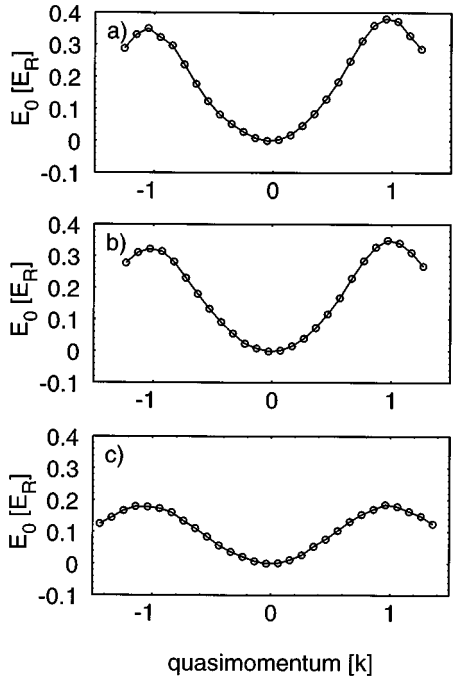

FIG. 5. Experimental determination of the fundamental energy band for (a) $U_0=1.4E_R$, (b) $2.3E_R$, (c) $4.4E_R$. This determination is obtained by integrating the mean velocity over quasimomentum [Eq. (9)].

C. Results in the accelerated frame

We have already presented Bloch oscillations in the fundamental band ($n=0$) in [8]. For sake of completeness the evolution of the Bloch states in the time domain $|n=0,q(t)\rangle$ and the oscillation of the mean velocity $\langle v\rangle_0(q)$ are recalled in Fig. 4. In these experiments, the acceleration a is -0.85 m/s^2 and $\tau_B=2\hbar k/ma=8.2$ ms. Such value of the period is several orders of magnitude longer than in solid-state systems. From these data it is possible to experimentally determine the shape of the fundamental band $E_0(q)$ by integrating the mean velocity over quasimomentum, as indicated by Eq. (9). The measured bands for different values of the potential depth are presented in Fig. 5. Note the very different radii of curvature of the band near $q=0$ and $q=\pm k$ for weak potentials [5(a) and 5(b)] and the flattening of the band as the potential depth U_0 increases.

BO can also occur in excited bands and we have observed these oscillations in the first excited band ($n=1$) as follows: we prepare atoms in the state $|n=1,q_0\simeq-0.5k\rangle$ by introducing a constant frequency shift so that atoms have a velocity $1.5v_R$ in the standing-wave frame. The subsequent acceleration is equal to -0.85 m/s^2, as for the oscillations in the fundamental band. In Fig. 6 the full momentum distribution in the accelerated frame is displayed for various times between 0 and τ_B and a potential depth $U_0=9.5E_R$. As in the fundamental band, the time evolution is periodic but the Bloch states display a richer structure. The initial distribution is mostly a combination of two plane waves $|1.5\hbar k\rangle$ (dominant) and $|-0.5\hbar k\rangle$. At $t_a=\tau_B/4$ the quasimomentum arrives at the avoided crossing with the second excited band and the corresponding Bloch state $|n=1,q=0\rangle$ is predominantly a superposition of the two plane waves $|-2\hbar k\rangle$ and $|2\hbar k\rangle$

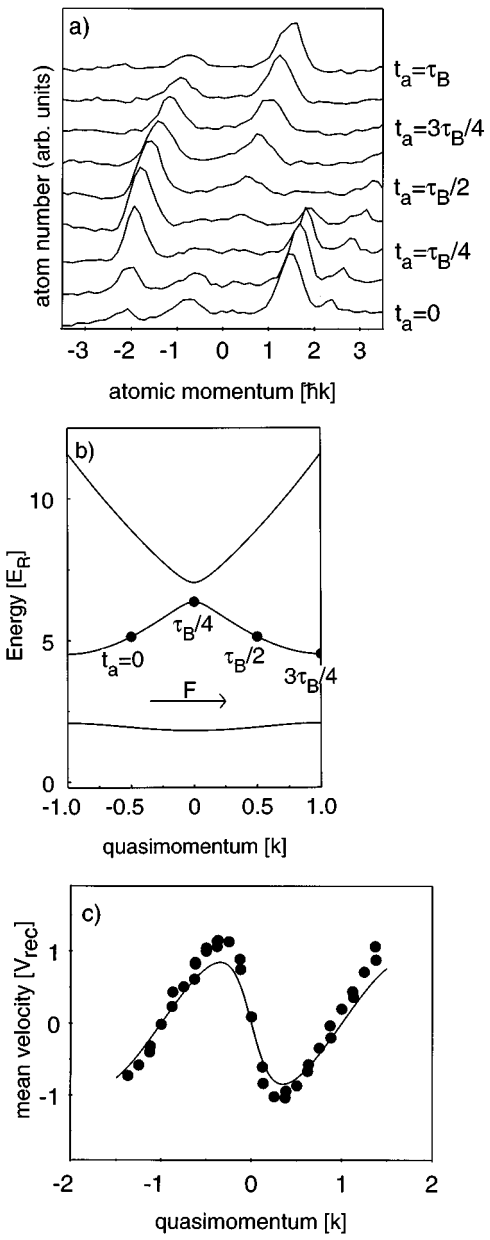

FIG. 6. Bloch oscillations of atoms in the first excited band. Before turning on the optical potential, the atoms are prepared with a momentum of $1.5\hbar k$. (a) Momentum distribution of Bloch states in the accelerated frame for equidistant values of the acceleration time t_a between $t_a=0$ and $t_a=\tau_B=8.2$ ms. (The small peak between 2 and $3\hbar k$ is an artifact due to a stray reflection on a cell window.) (b) Band structure and time evolution of the quasimomentum. (c) Mean atomic velocity. The light potential depth is $U_0=9.5E_R$ and the acceleration is $a=-0.85$ m/s^2. Solid line: theory with no adjustable parameter. Note the sign difference of the mean velocity for the oscillation in the first excited band and in the fundamental band [Fig. 4(b)].

with equal weights. In the further evolution, the weight of the component near $2\hbar k$ vanishes while the component near $-2\hbar k$ grows. After $3/4\tau_B$ the zone boundary $q=k$ is reached and the atom is in a superposition of momentum states with $-\hbar k$ and $\hbar k$. Finally this latter momentum peak grows and after one Bloch period the initial distribution is recovered. Note in addition that, at $t_a=0$, a third small peak is visible around $-2.1\hbar k$. We attribute the existence of this peak to the finite initial width of the momentum distribution [$0.6\hbar k$ full width at half maximum (FWHM) in these data] which is not very small as compared to $\hbar k$. During the adiabatic turn on of the optical potential, atoms in the wing of the distribution, having an initial momentum p close to $2\hbar k$ couple to a Bloch state which is a linear superposition of two plane waves at $|p\rangle$ and $|p-4\hbar k\rangle$. This finite width effect is also responsible for the slight curvature in the time evolution of the peaks in Fig. 6(a).

In Fig. 6(c), we also present the evolution of the mean velocity in the $n=1$ band for a value of the potential depth $U_0=9.5\ E_R$. This mean velocity is calculated in the same way as described in [8]. The amplitude of the velocity oscillations is greater than in the fundamental band and is $1.1v_R$ for $U_0=9.5\ E_R$. The agreement with the theoretical curve obtained from a numerical calculation of the band structure (shown in solid line) is good. Note also that for an identical applied force, the slopes around $q=0$ and $q=\pm k$ of the mean velocity in the excited and fundamental bands have opposite signs. This is expected from Fig. 3(b): to a minimum of the fundamental energy band corresponds a maximum of the excited band and vice versa. For values of $U_0<5E_R$—where we have observed BO in the fundamental band—the energy gap between the first and second excited bands is small and adiabatic evolution in the first band is difficult to obtain.

To conclude this section, we would like to underline that BO are a pure quantum effect which comes from the wave nature of the atoms. Here a matter wave is diffracted by a light structure, a situation entirely symetrical to the ordinary Bragg diffraction of light by matter lattice, as first pointed out in [2]. As for light diffraction, the wavelike atoms strongly interact with the potential, for special values of the wave vector. In the case of a weak potential where the Bloch states are very close to pure plane waves, we can give a simple description of BO. An atomic plane wave, initially prepared with momentum $p\simeq 0$, is accelerated by an external force. The momentum p increases linearly according to Newton's law until it reaches a critical value satisfying the Bragg condition $k_{at}=jk$, where $k_{at}=p/\hbar$, is the atomic wave vector and j is an integer. The atomic wave is then reflected and its momentum is reversed. The further evolution is nothing but the repetition of that process: an acceleration by the force followed by a Bragg reflection. This effect is illustrated in Fig. 4 for the fundamental band. In the case of the first excited band (Fig. 6), the oscillations result from two successive Bragg reflections. The first one corresponds to a second-order Bragg transfer of $-4\hbar k$ (from $|p=+2\hbar k\rangle$ to $|p=-2\hbar k\rangle$), while the second one leads to a change by $+2\hbar k$, a first-order Bragg reflection.

IV. BLOCH OSCILLATIONS: A QUANTUM-OPTICS APPROACH

While our experimental results can be perfectly explained using the Bloch formalism in the accelerated frame to describe the motion of atoms in the optical lattice in the presence of a constant inertial force, we would like to present here a different physical picture that is equally well suited to describe our experiment. We remain in the laboratory frame

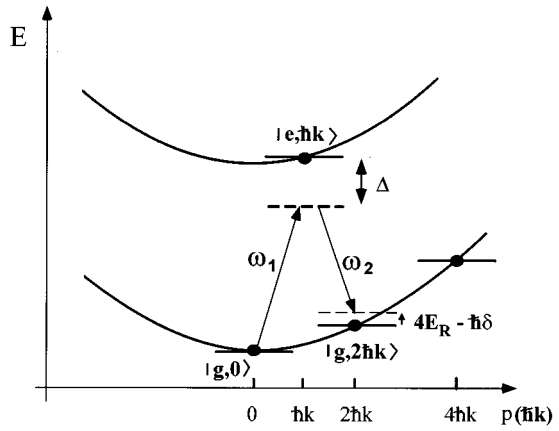

FIG. 7. Energy-momentum states in the laboratory frame. In the chirped standing wave, an initial state $|g,p\rangle$ is only coupled to $|g,p\pm 2j\hbar k\rangle$, where j is an integer, by stimulated two-photon Raman transitions.

and we deal with free atoms interacting with two counterpropagating laser waves having a time-dependent frequency difference.

A. Bloch oscillations as adiabatic rapid passage between momentum states

In the absence of spontaneous emission the atoms momentum can change by units of $\hbar(k_1-k_2)\approx 2\hbar k$ by absorbing a photon from one wave and emitting it into the other in a stimulated way, as depicted in Fig. 7. Because the atoms are initially prepared with a momentum spread much smaller than $2\hbar k$ and with a kinetic energy near zero, their possible states after interaction with the light fields are discrete points $|p=2j\hbar k, E=4j^2E_R\rangle$ $(j=0,1,2,3\ldots)$ on the momentum-energy parabola of the free particle [26] (cf. Fig. 7). The gain in kinetic energy is provided by the frequency difference between the two laser waves: the atoms are accelerated in the direction of the beam with the higher frequency by absorbing photons from it and reemitting low-frequency photons into the other. The transition $|p=2j\hbar k, E=4j^2E_R\rangle \rightarrow |p=2(j+1)\hbar k, E=4(j+1)^2E_R\rangle$ is resonant for an angular frequency difference $\Delta\omega=4(2j+1)E_R/\hbar$. As we start with the atoms at rest $(j=0)$ and $\Delta\omega=0$, these resonances are encountered sequentially and a gain of atomic momentum of $2\hbar k$ can be expected after each change in the frequency difference of $8E_R/\hbar$, as shown in Fig. 8. For a constant change in the angular frequency difference $\Delta\omega$ with the rate $\Delta\dot{\omega}$, the time required for this is

$$t=8E_R/\hbar\Delta\dot{\omega}=4E_R/\hbar ka=2\hbar k/ma, \tag{14}$$

which is equal to the Bloch period for the inertial force $ma=m\Delta\dot{\omega}/2k$. Thus the mean atomic velocity increases by $2\hbar k/m$ during each Bloch period. As shown in Fig. 8(b), the Bloch oscillations in the laboratory frame appear as a periodic deviation of the mean velocity around the linear increase in time at. The method of exciting the transition between two energy levels with a electromagnetic wave of variable detuning that is scanned through resonance is well known under the term adiabatic rapid passage (ARP) [27].

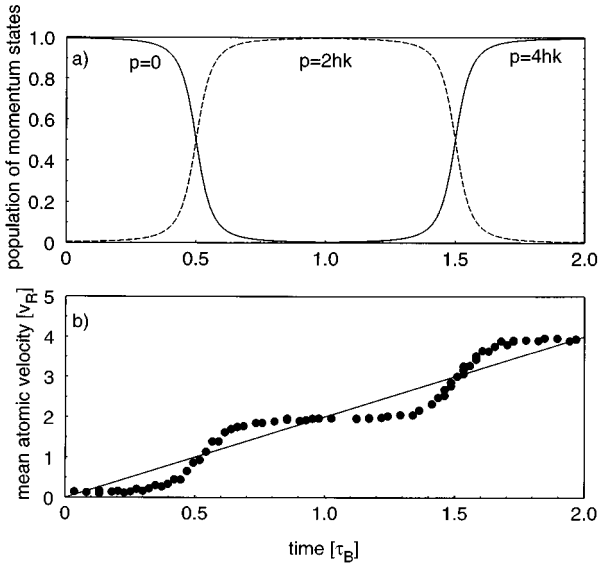

FIG. 8. (a) Population of momentum states $|p=2j\hbar k\rangle$ as a function of time in the chirped standing wave (numerical simulation). (b) Experimental measurement of the mean atomic velocity in the laboratory frame as a function of time. Parameters are the same as in Fig. 4.

For properly chosen parameters (i.e., a scan range that is greater than the peak Rabi frequency Ω and slow enough rate of change of the detuning $\Delta\dot{\omega}\ll\Omega^2$) the transfer between the states is complete and the method can be used to efficiently create an inversion between the levels. In our case a sequence of transfers between momentum states results in a coherent acceleration of the atoms in the laboratory frame.

Multiple ARP is a powerful method in quantum physics. For instance, a sequence of ARP has been used to produce Rydberg atoms in circular states [28]. Multiple ARP, as a means of momentum transfer between light and atoms, has already been proposed long ago, but considering the excitation and deexcitation of an internal state of the atom using a one-photon transition [29]. For instance, they occur in saturation spectroscopy with curved wave fronts [30]. Our system has some peculiarities in comparison with previous studies of ARP: the states are linked by a two-photon transition; internal states of the atom are not excited, consequently there is no relaxation or dissipation; the sequence of levels is infinite, so that a large number of successive transfers can be made. This dynamical case has to be contrasted with the single two-photon transfer occuring in the recoil-induced resonances observed in dissipative optical lattices in which the atomic momentum spread is larger than $2\hbar k$ [18,31].

The two-photon Raman process can be characterized by an effective Rabi frequency

$$\Omega=\Omega_1\Omega_2/2\Delta=U_0/2\hbar, \tag{15}$$

which is proportional to the depth of the light-shift potential (Ω_1,Ω_2: Rabi frequencies of the two beams, Δ: detuning from the atomic resonance line). The two ARP conditions then read $\Delta\dot{\omega}\ll\Omega^2\ll 64E_R^2/\hbar^2$ and are well fulfilled for the conditions of our BO experiment in the fundamental energy band. The second condition, which is equivalent to the weak binding limit for the periodic potential, allows us to treat the

transitions sequentially and to take only two momentum states at a time. The first condition, which ensures the adiabaticity of the process, is equivalent to avoiding interband transitions in the band-structure model. It will be discussed quantitatively in the following paragraph.

The model of ARP between momentum states is also able to predict, quantitatively, the temporal behavior of the BO, i.e., of the mean velocity in the laboratory frame $\langle v\rangle_{\mathrm{lab}}(t)$. Focusing now on one of the momentum transfers displayed in Fig. 8, we consider only two states at a time and the mean velocity is simply given by

$$\langle v\rangle_{\mathrm{lab}}(t)=\frac{2\hbar k}{m}[jP_{2j}(t)+(j+1)P_{2(j+1)}(t)], \qquad (16)$$

where P_{2j} is the time-dependent probability of finding the atom in momentum state $|2j\hbar k\rangle$. These probabilities can be calculated from the vector model of the optical Bloch equations [32]

$$P_{2(j+1)}=\frac{1}{2}+\frac{\delta}{2\sqrt{\delta^2+\Omega^2}}, \quad P_{2j}=1-P_{2(j+1)}, \qquad (17)$$

where

$$\delta=\Delta\omega-4(2j+1)E_R/\hbar \qquad (18)$$

is the detuning from the two-photon resonance. For small values of Ω, $\langle v\rangle_{\mathrm{lab}}(t)$ changes very little during the first half period ($-4E_R/\hbar\leqslant\delta<0$) and makes an abrupt jump of $2\hbar k/m$ as the resonance $\delta=0$ is encountered. This corresponds to a BO with the maximal amplitude in velocity of $\hbar k/m$. For larger values of Ω, which corresponds to stronger binding of the atoms in the periodic potential, the increase in $\langle v\rangle_{\mathrm{lab}}(t)$ approaches a linear behavior in δ or in time, namely, the amplitude of the BOs vanishes. Obviously this simple model cannot be extended to arbitrarily strong coupling, because the approximation of having only two momentum states involved at a time breaks down. In that case, we have solved numerically the Schrödinger equation involving a large set of momentum states. Note that for any value of the lattice potential these results are identical to those obtained with the Bloch approach presented in Sec. III. The full equivalence between the two descriptions is demonstrated in the Appendix. A similar quantum-optics approach has been independently developed for atomic three-level and two-level systems [33].

To compare the experimental results to the simple two-state model [Eq. (17)] we have plotted, in Fig. 9, the height of the peak at $|2\hbar k\rangle$ for the first Bloch period as a function of the detuning and for different values of Ω, i.e., of the potential depth U_0. We find that the experimental data can be well fitted by Eq. (17), but with Rabi frequencies about 12% smaller than those deduced from the measured intensities. This slight discrepancy may be attributed to an error in absolute power calibration, as well as to the transverse spread of the atomic cloud in the Gaussian profile of the laser beams during the $\sim$20 ms interaction time.

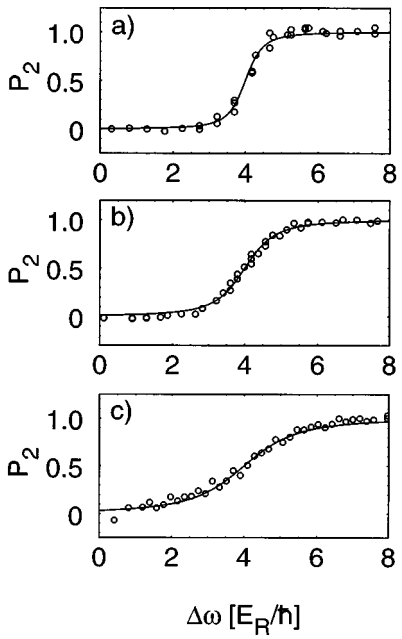

FIG. 9. Probability of finding the atom in momentum state $2\hbar k$ as a function of the detuning from the two-photon resonance δ for various effective Rabi frequencies. Solid lines are results from the two-state model of adiabatic rapid passage between momentum states [cf. Eq. (17)]. (a) $U_0=1.4E_R$, (b) $U_0=2.3E_R$, (c) $U_0=4.4E_R$.

B. Dressed-atom picture

Another interesting viewpoint can be given with the dressed-atom approach [34], in which the state of the system is described by $|p,N_1,N_2\rangle$, where p is the momentum of the atom, N_1 is the number of photons in the laser wave of frequency ω_1, and N_2 the number of photons in the laser wave of frequency ω_2. With redistribution processes, the state $|p,N_1,N_2\rangle$ is coupled to the states $|p\pm 2j\hbar k,N_1\mp j,N_2\pm j\rangle$. For our initial condition $p=0$ and $N_1=N_2=N_0$, with a momentum spread $\delta p\ll\hbar k$, the system evolves in the space subtended by the states $|j\rangle=|2j\hbar k,N_0-j,N_0+j\rangle$. Without the coupling between the atom and the laser waves, the energy of state $|j\rangle$ for a frequency difference $\omega_1-\omega_2=\Delta\omega$

$$E_j(\delta)=4j^2E_R+N_0\hbar(\omega_1+\omega_2)-j\hbar\Delta\omega. \qquad (19)$$

The effect of a weak coupling ($U_0\ll E_R$) is significant only when two states $|j\rangle$ are degenerate: the crossings in Fig. 10 become avoided crossings. By adiabatically switching on the beams in our experiment, we prepare the system in an eigenstate. Then, when the frequency difference $\omega_1-\omega_2$ is slowly increased (assuming for simplicity that $\omega_1+\omega_2$ remains constant), the system follows adiabatically the evolution of the eigenstate, leading to a series of momentum changes. If the initial frequency difference is zero, the momentum of the atoms is periodically increased by $2\hbar k$ at each of the first-order anticrossings in Fig. 10(a): this is the signature in the laboratory frame of Bloch oscillations in the fundamental band. With an initial frequency difference of $6E_R/\hbar$, we prepare the atoms with a momentum $1.5\hbar k$ in the standing-wave frame [Fig. 10(b)]. During the frequency chirp, the

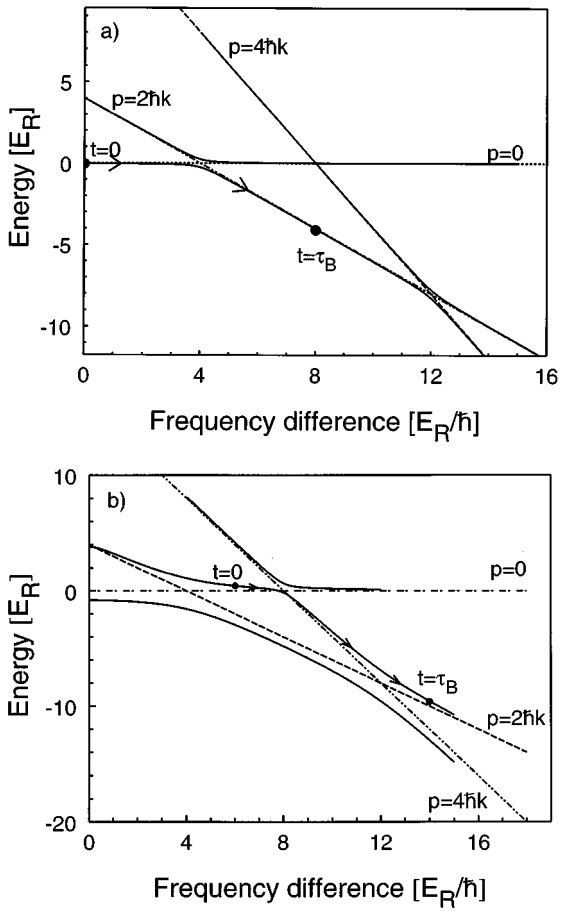

FIG. 10. Bloch oscillations in the dressed atom basis. The straight lines represent the eigenenergies of the system atom+laser fields as a function of the frequency difference between the two counterpropagating waves in the absence of coupling. The effect of a weak coupling is to lift the degeneracy at the line crossings and to produce new eigenenergies. (a) For $U_0=E_R$, only the first-order anticrossing at $4E_R/\hbar$ is visible. When the difference frequency is increased from 0, atoms at t=0 with $|p=0\rangle$ may follow adiabatically the lower-energy curve and thus gain a momentum of $2\hbar k$ when the frequency difference is $4E_R$. After a time τ_B the frequency difference is $8E_R$. This corresponds to one Bloch oscillation in the fundamental band. This process can be repeated periodically whenever the frequency difference equals $4[j^2-(j-1)^2]$, where j is an integer greater than 1. This results in a coherent momentum transfer to the atoms in the laboratory frame and, hence, to an acceleration of the atomic cloud. (b) $U_0=5E_R$. The first-order anticrossing and a higher-order anticrossing at $8E_R/\hbar$ are significant. If the atoms are prepared at $t=0$ in the upper-energy branch (for instance with a frequency difference of $6E_R$), the first anticrossing at a frequency difference of $8E_R$ transfers $+4\hbar k$ of momentum to the atoms. The second anticrossing at $12E_R$ reduces the atom momentum by $2\hbar k$ resulting in a total transfer of $2\hbar k$ after one Bloch period. This is the equivalent of the Bloch oscillations in the first excited band.

momentum of the atoms is first increased by $4\hbar k$ at the anticrossing which corresponds to a frequency difference of $8E_R/\hbar$ and which is a four-photon process. Then the momentum is decreased by $2\hbar k$ at a frequency difference of $12\hbar k$ by a first-order anticrossing. This evolution corresponds to the Bloch oscillations in the first excited band.

V. PREPARATION OF ULTRACOLD ATOMIC BEAMS

Using the moving periodic potential of the detuned laser beams a large number of photon momenta can be transferred to the atoms coherently, accelerating them without any dissipation or heating. With this technique, we are able to produce an atomic beam with very small (i.e., subrecoil) momentum spread in the beam direction. This may find applications in precision experiments, where very well defined velocities are desirable, for instance, in atomic fountain clocks [35] or in atom transport and interferometry. For practical applications the most important figure of merit is the maximal acceleration under which the atoms stay bound to the potential. This determines the maximal velocity that can be reached in a given interaction time for atoms starting at rest.

Classically, a periodic potential $U_0\sin^2 kz$ would be tilted under the influence of the inertial force $-ma$. Acceleration is possible up to a critical value $a_{cl}=U_0k/m$, from where on there exist no more local potential minima that can bind the particles. In a quantum treatment the requirement for acceleration is that the atoms stay in the fundamental band and do not perform transitions to higher-energy bands. In the band structure of the potential $U_0\sin^2 kz$, which is in our experiments smaller than $\sim 20E_R$, the widths of the band gaps between the nth and the $(n+1)$th band diminish with n. Since the probability for interband transitions increases exponentially with diminishing width of the band gap, an atom that has passed the first and largest band gap, and has made the transfer from the fundamental to the first excited band, will also make the transitions to higher bands and finally reach the continuum [36]. When the quasimomentum scans the Brillouin zone, the critical moment for interband transitions is at the zone boundary $q=k$, where the first excited band approaches the fundamental band the most. This is encountered once during each Bloch period. We suppose a transition rate per Bloch period given by a Landau-Zener formula [37]

$$r=\exp(-a_c/a), \tag{20}$$

where the critical acceleration a_c is proportional to the square of the band gap between the fundamental and the first excited band, which in the limit of weak binding is proportional to the potential depth U_0. Here we have

$$a_c/a=\pi\Omega^2/2\Delta\dot{\omega}. \tag{21}$$

We determined these transition rates experimentally by accelerating atoms, initially cooled to a subrecoil momentum spread, for a fixed time $t_0=n\tau_B$ and by measuring the fraction of atoms that reached the final velocity $v=at_0$ for different values of a and U_0. Typical transition rates were in the range 2–20 % and followed well the exponential behavior expected after the Landau-Zener formula. As an example of the data we show in Fig. 11 the initial momentum distribution and that obtained after a transfer of 30 $\hbar k$ in 1.4 ms ($a=76$ m/s^2) in a potential $U_0=9.5E_R$, leading to a total efficiency of 60% or a transition rate $r=0.033$.

The extrapolated values for the critical acceleration a_c are plotted in Fig. 12 as a function of U_0. The critical acceleration is measured in units of $a_0=\hbar^2k^3/m^2$, which is equal to

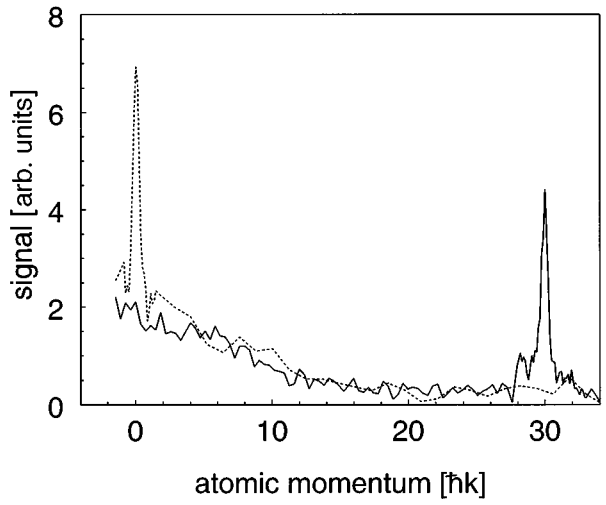

FIG. 11. Determination of the critical acceleration by coherent acceleration of atoms with a subrecoil momentum spread of $\hbar k/4$. $U_0=9.5E_R$ and the acceleration is 76 m/s^2. Dotted line: initial distribution. Solid line: 30 photon recoils are transfered after 1.4 ms of acceleration. From these data we deduce a total transfer efficiency of 60% and a Landau-Zener loss rate per Bloch period of 0.033.

91.6 m/s^2 for the cesium atom. For the range of potential depths investigated here ($U_0<10E_R$) the relation between a_c and U_0 is well fitted by

$$\frac{a_c}{a_0}=0.037\left(\frac{U_0}{E_R}\right)^2. \tag{22}$$

Our numerical value of 0.037 is in reasonable agreement with the value $\pi/64\approx 0.049$ derived from Eq. (21), considering our 30% laser intensity uncertainty.

The greatest momentum transfer we could measure in the experiment was $112\hbar k$, being limited by the laser power available for the optical potential and by the geometry of our detection system, which was designed to probe atoms nearly at rest and close to the position of the MOT. Numerical band-structure calculations indicate that the proportionality

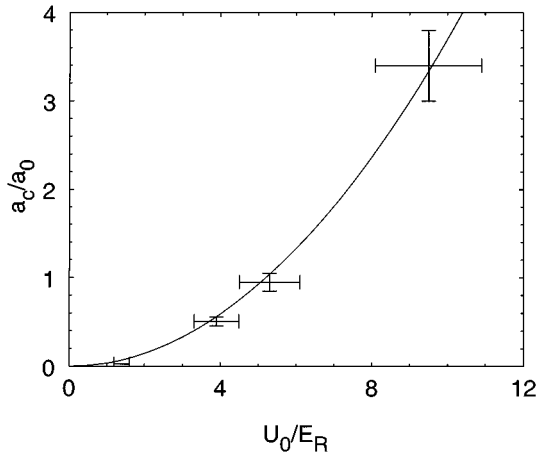

FIG. 12. Critical acceleration as a function of laser intensity. Solid line: fit with $a_c/a_0=0.037(U_0/E_R)^2$. The critical acceleration depends quadratically on the potential depth U_0 for $U_0\leqslant 10E_R$. $a_0=\hbar^2k^3/m^2=91.6$ m/s^2 for cesium.

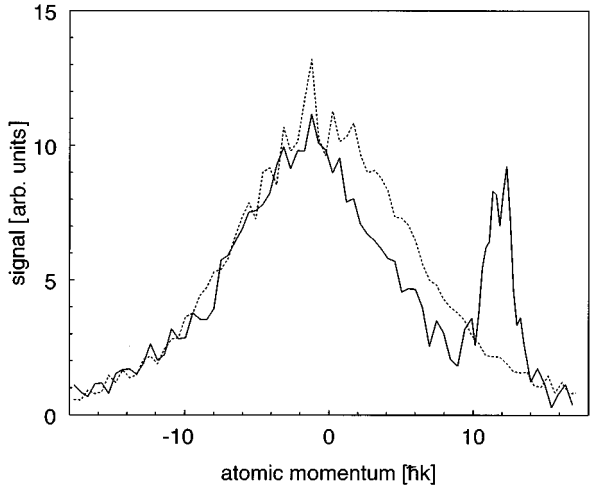

FIG. 13. Acceleration of a molasses momentum distribution with $U_0=8.3E_R$ and $a=3.5$ m/s$^2=0.015a_c$: from a distribution of full width $\sim 10\hbar k$ (dotted line), only a peak having a width of $2\hbar k$ is efficiently transfered to higher momenta (here $12\hbar k$). Note also the $-2\hbar k$ shift of the positive side of the momentum distribution whereas the momenta opposed to the direction of the acceleration remained unchanged after the acceleration (see text).

between U_0 and the band gap holds up to $U_0\approx 15E_R$. At this value of U_0 for cesium an acceleration of 70.4 m/s^2 leads to a Bloch period of 0.1 ms and a transition rate $r=2\times 10^{-5}$, so that during a 10 ms interaction time, 200 $\hbar k$ can be transferred to 99.8% of the atoms, leading to a final velocity of 0.7 m/s. This acceleration method is particularly simple and may find interesting applications in atomic fountains largely used in high-precision measurements. Note that due to the scaling of a_0 with k^3/m^2, significantly higher velocities are possible with lighter atoms and shorter wavelengths. This simple method might also be an interesting alternative to the atom interferometer method for measuring the photon recoil and thus h/m in frequency units [38].

In the case of strong binding (i.e., for $U_0>20E_R$) the first band gap continues to increase, but slower than linearly with U_0. Here the Landau-Zener theory is not applicable any more because the lowest bands become essentially flat (independent of q). The notion of a level crossing at the zone boundary has no meaning any longer and higher-order level crossings cannot be ignored.

This technique of acceleration by a moving periodic potential cannot only be applied to atoms cooled to subrecoil energies, but also to ensembles of atoms having a larger momentum spread. In the Bloch picture, the atoms will be spread over several Brillouin zones, or energy bands, of the periodic potential. During the adiabatic turn on of the potential, only atoms with an initial momentum in the range $-\hbar k<p<\hbar k$ are prepared in the fundamental energy band. For large values of the acceleration, only these atoms will fulfill the adiabaticity condition for BO and will undergo Bloch oscillations. They will be efficiently accelerated in the laboratory frame. After the acceleration phase, one expects a peak of atoms around the final velocity having the height of the initial distribution around $p=0$ and with a width of $2\hbar k$. Figure 13 shows the experimental result for an initial momentum distribution having a rms momentum spread of about $5\hbar k$, obtained by cooling the atoms in optical molas-

ses. A momentum transfer of $12\hbar k$ was performed in a potential of depth $U_0 = 8.3E_R$ and using an acceleration of 3.5 m/s^2 or $0.015a_c$. Note that this simple selection method produces an atomic beam with a longitudinal momentum spread of only $\sim 2\hbar k$, narrower than that attainable with polarization gradient cooling methods.

This figure presents another interesting feature. At first glance, one would expect also a hole of width $\sim 2\hbar k$ in the molasses distribution corresponding to the atoms efficiently accelerated. Actually this is not the case. Consider first the negative side of the two momentum distributions. Below $-\hbar k$ the two distributions coincide, indicating that the acceleration phase has not affected these atoms. The atoms with an initial momentum outside of the first Brillouin zone and with $p \leqslant -\hbar k$, i.e., opposed to the direction of acceleration, are prepared in excited bands during the adiabatic turn on of the potential. During the acceleration phase the adiabatic criterion for BO is not fulfilled for these bands and the atoms are passing diabatically to higher bands and then to the continuum. They are essentially unperturbed by the optical potential. On the other hand, the atoms in the positive wing of the velocity distribution with $p \geqslant \hbar k$ are faster than the moving potential at the beginning of the acceleration phase. Their quasimomentum descend in the band structure. When they encounter the crossing between the fundamental and the first excited band they pass it adiabatically, i.e., they loose $2\hbar k$ in the laboratory frame. After this momentum transfer, the atoms evolve similarly to the ones initially having a negative velocity: they are no longer perturbed by the potential. This $-2\hbar k$ shift is clearly visible on the positive side of the momentum distribution in Fig. 13.

In the picture of adiabatic rapid passage between momentum states in the laboratory frame, the atoms with $|p| < \hbar k$ will experience the normal sequence of ARP and their momentum will be increased by $12\hbar k$. Atoms with an initial momentum lower than $-\hbar k$ will never encounter the resonance condition for ARP. They are left unchanged during the acceleration phase. On the other hand, atoms with an initial momentum greater than $\hbar k$ will experience one ARP when the resonance condition is fulfilled. This ARP decreases their momentum by $2\hbar k$ and in the subsequent evolution they evolve like the atoms having initially a negative momentum: they no longer interact with the chirped wave.

VI. SUMMARY

In this paper, we have shown that atoms in a light lattice constitute a good model system for the study of quantum effects usually described in solids, such as Bloch oscillations. Thanks to our ability to prepare atoms with a small momentum spread and to the possibility to easily switch on and off light fields in a controlled way, we have been able to directly observe the momentum distribution of Bloch states and Bloch oscillations in the time domain for the first two energy bands. We have given a quantum-optics interpretation of these phenomena in terms of adiabatic rapid passage between momentum states. Applications to atomic beam coherent manipulation, atom transport, and high-precision measurement of h/m have been outlined.

ACKNOWLEDGMENTS

We are grateful to C. Cohen-Tannoudji, G. Grynberg, G. Bastard, J. Dalibard, and M. Raizen for stimulating discussions. E.P. acknowledges support from the European Union through the HCM program. This work was supported in part by NEDO, CNES, and Collège de France. Laboratoire Kastler Brossel is Unité de Recherche de l'Ecole Normale Supérieure et de l'Université Pierre et Marie Curie, associée au CNRS.

APPENDIX

Several Hamiltonians are used in this paper to analyze the atomic motion in the accelerated optical standing wave. The first one corresponds to the reference frame of the laboratory

$$H_{\mathrm{lab}}(t) = \frac{p^2}{2m} + U_0 \sin^2\left[kx - \frac{1}{2}(\phi_+(t) - \phi_-(t)) \right], \tag{A1}$$

where

$$\phi_+(t) - \phi_-(t) = \int_0^t d\tau \Delta\omega(\tau), \tag{A2}$$

$$= k(at^2 - 2v_0 t) \tag{A3}$$

is the phase difference between the two laser running waves. The sign of v_0 is chosen in accordance with Sec. III B. The potential in Eq. (A1) corresponds to the light shift induced by a laser field proportional to $\exp\{i[kx - \phi_+(t)]\} - \exp\{i[-kx - \phi_-(t)]\}$.

The second Hamiltonian holds in the accelerated frame and is time independent,

$$H_{\mathrm{acc}} = \frac{p^2}{2m} + U_0 \sin^2 kx + max. \tag{A4}$$

We identify, in this Appendix, the unitary transformation $U(t)$ linking these two Hamiltonians, i.e., we solve the equation

$$H_{\mathrm{acc}} = U(t) H_{\mathrm{lab}}(t) U(t)^\dagger + i\hbar \left(\frac{d}{dt} U(t) \right) U(t)^\dagger. \tag{A5}$$

Intuitively the effect of $U(t)$ is to perform a translation in position space of $\alpha(t) = at^2/2 - v_0 t$ and a translation in momentum space of $\beta(t) = m(at - v_0)$, corresponding to the classical change of coordinates defining the accelerated frame. This motivates the ansatz

$$U(t) = e^{i\alpha(t)p/\hbar} e^{-i\beta(t)x/\hbar} e^{i\gamma(t)/\hbar}, \tag{A6}$$

where $\gamma(t)$ is to be determined.

From Eq. (A6) we immediately get

$$U(t) x U(t)^\dagger = e^{i\alpha(t)p/\hbar} x e^{-i\alpha(t)p/\hbar}, \tag{A7}$$

$$= x + \alpha(t), \tag{A8}$$

$$U(t) p U(t)^\dagger = e^{-i\beta(t)x/\hbar} p e^{i\beta(t)x/\hbar}, \tag{A9}$$

$$= p + \beta(t). \tag{A10}$$

The inertial term [last term of Eq. (A5)] is obtained as follows:

$$i\hbar\left(\frac{d}{dt}U(t)\right)U(t)^{\dagger}=-\dot{\alpha}(t)p+\dot{\beta}(t)U(t)xU(t)^{\dagger}-\dot{\gamma}(t), \tag{A11}$$

$$=-(at-v_0)p+max+\frac{1}{2}ma^2t^2$$

$$-mav_0t-\dot{\gamma}(t). \tag{A12}$$

For the choice $\gamma(t)=ma^2t^3/3-mav_0t^2+mv_0^2t/2$ one can then easily check that the relation (A5) holds.

A third type of transformation may be considered to unify the various points of view of this paper. It merely consists in a translation of Eq. (A1) in position space followed by a global change of phase

$$\mathcal{U}(t)=e^{i\alpha(t)p/\hbar}e^{-i\eta(t)/\hbar}. \tag{A13}$$

For the choice $\eta(t)\equiv 0$ this unitary transformation leads to

$$H_{QO}(t)=\frac{p^2}{2m}-(at-v_0)p+U_0\sin^2kx, \tag{A14}$$

$$=\frac{p^2}{2m}-\Delta\omega(t)p/2k+U_0\sin^2kx, \tag{A15}$$

which, up to the additive constant term $N_0\hbar(\omega_1+\omega_2)$, has the same spectrum as the one obtained in the dressed-atom approach, i.e., in the ''quantum-optics'' point of view. For the other choice, $\eta(t)=ma^2t^3/6-mav_0t^2/2+mv_0^2t/2$ this unitary transformation leads to

$$H_{SSP}(t)=\frac{[p-m(at-v_0)]^2}{2m}+U_0\sin^2kx, \tag{A16}$$

$$=\frac{[p+\hbar q(t)]^2}{2m}+U_0\sin^2kx, \tag{A17}$$

which is exactly the Hamiltonian of Eq. (7) for the periodic part of the wave function $|u(t)\rangle$, i.e., in the ''solid-state physics'' point of view.

[1] See, e.g., *Laser Manipulation of Atoms and Ions*, Proceedings of the International School of Physics ''Enrico Fermi,'' edited by E. Arimondo, W. Phillips, and F. Strumia (North-Holland, Amsterdam, 1992).

[2] P. L. Gould, G. A. Ruff, and D. E. Pritchard, Phys. Rev. Lett. **56**, 827 (1986); P. J. Martin, B. G. Oldaker, A. H. Miklich, and D. E. Pritchard, *ibid.* **60**, 515 (1988).

[3] For a recent review see, C. S. Adams, M. Sigel, and J. Mlynek, Phys. Rep. **240**, 143 (1994).

[4] E. Rasel, M. Oberthaler, H. Batelaan, J. Schmiedmayer, and A. Zeilinger, Phys. Rev. Lett. **75**, 2633 (1995); D. M. Giltner, R. W. McGowan, and S. A. Lee, *ibid*. **75**, 2638 (1995).

[5] F. L. Moore, J. C. Robinson, C. Bharucha, P. E. Williams, and M. G. Raizen, Phys. Rev. Lett. **73**, 2974 (1994).

[6] M. Kasevich and S. Chu, Phys. Rev. Lett. **69**, 1741 (1992).

[7] J. Reichel, F. Bardou, M. Ben Dahan, E. Peik, S. Rand, C. Salomon, and C. Cohen-Tannoudji, Phys. Rev. Lett. **75**, 4575 (1995).

[8] M. Ben Dahan, E. Peik, J. Reichel, Y. Castin, and C. Salomon, Phys. Rev. Lett. **76**, 4508 (1996).

[9] S. Wilkinson, C. Bharucha, K. Madison, Qian Niu, and M. Raizen, Phys. Rev. Lett. **76**, 4512 (1996); Qian Niu, Xian-Geng Zhao, G. Georgakis, and M. Raizen, *ibid*. **76**, 4504 (1996).

[10] F. Bloch, Z. Phys. **52**, 555 (1929).

[11] C. Zener, Proc. R. Soc. London Ser. A **145**, 523 (1934).

[12] E. Mendez and G. Bastard, Phys. Today **46** (6), 34 (1993).

[13] For a metal with $a=0.1$ nm and an electric field of 10^{-2} V/cm the Bloch period is equal to 41 μs whereas a typical relaxation time is on the order of 10 fs. In a semiconductor superlattice the period is typically $a=10$ nm and the field can be as high as 10 kV/cm ($F\approx 10^{-13}$ N), leading to a Bloch period in the picosecond range. In our atomic system the lattice period is $a=426$ nm, the force typically on the order of 10^{-25} N and the corresponding Bloch period in the millisecond range.

[14] J. Feldmann, K. Leo, J. Shah, D. A. B. Miller, J. E. Cunningham, T. Meier, G. v. Plessen, A. Schulze, P. Thomas, and S. Schmitt-Rink, Phys. Rev. B **46**, 7252 (1992).

[15] K. Leo, P. Haring Bolivar, F. Brüggemann, R. Schwedler, and K. Köhler, Solid State Commun. **84**, 943 (1992).

[16] C. Waschke, H. Roskos, R. Schwedler, K. Leo, H. Kurz, and K. Köhler, Phys. Rev. Lett. **70**, 3319 (1993).

[17] For a recent review, see M. G. Prentiss, Science **260**, 1078 (1993).

[18] J.Y. Courtois, G. Grynberg, B. Lounis, and P. Verkerk, Phys. Rev. Lett. **72**, 3017 (1994).

[19] Closely related work is performed by the authors of Ref. [9] [M. Raizen (private communication)].

[20] C. Monroe, W. Swann, H. Robinson, and C. Wieman, Phys. Rev. Lett **65**, 1571 (1990).

[21] C. Salomon, J. Dalibard, W. Phillips, A. Clairon, and S. Guellati, Europhys. Lett. **12**, 683 (1990).

[22] J. Reichel, O. Morice, G. M. Tino, and C. Salomon, Europhys. Lett. **28**, 477 (1994).

[23] G. Santarelli, A. Clairon, S. N. Lea, and G. M. Tino, Opt. Commun. **104**, 339 (1994).

[24] See, e.g., N. W. Ashcroft and N. D. Mermin, *Solid State Physics* (Saunders, Philadelphia, 1976).

[25] A. Messiah, *Quantum Mechanics* (North-Holland, Amsterdam, 1962), Vol. 2.

[26] C. Bordé, in *Laser Spectroscopy 3*, edited by J. Hall and J. Carlsten (Springer-Verlag, Berlin, 1977), p. 121.

[27] A. Abragam, *The Principles of Nuclear Magnetism* (Oxford University Press, London, 1961).

[28] R. G. Hulet and D. Kleppner, Phys. Rev. Lett. **51**, 1430 (1983).

[29] I. Nebenzahl and A. Szöke, Appl. Phys. Lett. **25**, 327 (1974).

[30] C. Bordé, in *Frequency Standards and Metrology*, Proc. of the Fourth Symposium, edited by A. De Marchi (Springer, Berlin, 1989).

[31] D. Meacher, D. Boiron, H. Metcalf, C. Salomon, and G. Gryn-

berg, Phys. Rev. A, **50**, R1992 (1994).
[32] L. Allen and J. Eberly, *Optical Resonance and Two-level Atoms* (Wiley, New York, 1975).
[33] K. Marzlin and J. Audretsch, Phys. Rev. A **53**, 4352 (1996); Europhys. Lett. **36**, 43 (1996).
[34] See, e.g., C. Cohen-Tannoudji, J. Dupont-Roc, and G. Grynberg, *Atom-Photon Interactions* (John Wiley, New York, 1992), p. 407.
[35] A. Clairon, P. Laurent, G. Santarelli, S. Ghezali, S. Lea, and M. Bahoura, IEEE Trans. Instrum. Meas. **44**, 128 (1995).
[36] We neglect here possible returns from the second band to the first one, which may lead to additional interference effects.
[37] C. Zener, Proc. R. Soc. London Ser. A **137**, 696 (1932).
[38] D. Weiss, B. Young, and S. Chu, Phys. Rev. Lett. **70**, 2706 (1993).